Preprints of the 22nd IFAC World Congress
Yokohama, Japan, July 9-14, 2023

Wave-to-Wire Efficiency Maximisation for Oscillating-Water-Column Systems ⋆

Marco Rosati * **John V. Ringwood** **

* *Centre for Ocean Energy Research, Maynooth University, Maynooth, Co. Kildare, Ireland (e-mail: marco.rosati.2021@mumail.ie).*
** *Same address (e-mail: john.ringwood@mu.ie).*

Abstract:
Wave energy is a significant source of renewable energy which is harnessed by wave energy converters (WECs). However, due to the relatively high levelised cost of energy, wave energy has not attained a commercial stage yet. One of the key pathways to achieve commercialisation of WECs is to design effective control strategies to optimise the overall wave-to-wire (W2W) energy conversion process. This paper particularly focuses on W2W efficiency maximisation for oscillating-water-column (OWC) WECs. In OWC systems, the displacement of a water column compresses/decompresses a volume of air, consequently generating a bidirectional air flow. The air flow is typically used to drive a self-rectifying air turbine, which is directly coupled with a suitable electric generator. Due to the demanding issue of turbine efficiency, current OWC control strategies aim to maximise turbine efficiency by controlling the turbine rotational speed, albeit ignoring hydrodynamic performance. However, for Wells turbines, variations in the rotational speed affect the hydrodynamic efficiency (i.e., the wave-to-pneumatic energy conversion process) of the OWC system. Furthermore, the generator performance also depends on rotational speed and, therefore, rotational speed should be ideally modulated to improve the overall W2W efficiency, rather than just turbine efficiency. To this end, this paper investigates the benefits of W2W efficiency maximisation through Wells turbine rotational speed modulation, for a fixed OWC system. Results from numerical simulation show that, for Wells turbines, appropriate rotational speed control can further improve the overall OWC W2W energy conversion process, especially due to the impact of rotational speed on the hydrodynamic performance.

Keywords: Energy systems, hydrodynamic/aerodynamic interactions, oscillating-water-column, wave energy, wave-to-wire efficiency, Wells turbine.

1. INTRODUCTION

Wave energy is a significant source of renewable energy (Astariz and Iglesias, 2015) which can considerably contribute to decarbonization.

One of the most promising wave energy converters (WECs), which are devices used to harness wave power, is the oscillating-water-column (OWC) (Falcão and Henriques, 2016), shown in Fig. 1. Essentially, ocean waves excite a water column which consequently compresses and decompresses an air volume in a pneumatic chamber. The air compression/decompression generates a bidirectional air flow which is typically used to drive a self-rectifying air turbine (Falcão and Gato, 2012), such as a Wells turbine or an impulse-like turbine. Finally, the turbine is directly coupled to a suitable electric generator, which converts the turbine mechanical power into electrical power.

To date, WECs struggle to reach commercial viability due to the relatively high levelised cost of energy (LCoE) characterising wave energy projects, defined as

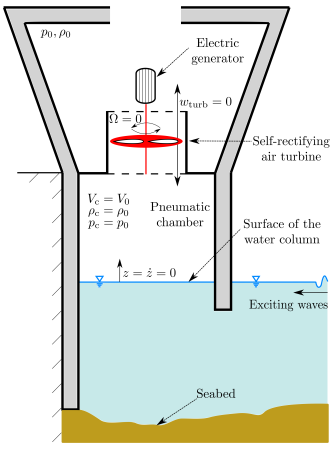

Fig. 1. Schematics of a fixed OWC device in still water conditions.

$$\text{LCoE} = \frac{\text{CapEx} + \text{OpEx}}{\text{Produced energy over the WEC lifetime}}, \quad (1)$$

where CapEx and OpEx indicate the capital and operational costs, respectively. To minimise the LCoE, comprehensive control strategies for maximising the produced

⋆ This paper is supported by MaREI, the SFI Research Centre for Energy, Climate and Marine, under grant No. 12/RC/2302_P2.

electric energy are essential (Chang et al., 2018), although energy maximisation alone does not necessarily imply a better return of investment (effects of control on CapEx and OpEx also need to be considered).

In OWC control, to obtain satisfactory levels of energy production, it is crucial to keep the turbine operating around its maximum efficiency point (MEP). Moreover, the lack of suitable actuators makes traditional WEC hydrodynamic control (Ringwood, 2020) (which, for OWC WECs, corresponds to the optimisation of the wave-to-pneumatic energy conversion process) more difficult for OWCs (Rosati and Ringwood, 2022). As such, OWC control strategies typically focus on turbine efficiency maximisation (Rosati et al., 2022a; Garrido et al., 2012; Henriques et al., 2019), ignoring the hydrodynamic/aerodynamic interaction, i.e., the effect of turbine rotational speed on hydrodynamic performance. Although, for impulse-like turbines, it is reasonable to neglect the effect of the hydrodynamic/aerodynamic interaction, this assumption is not realistic for Wells turbines (Rosati et al., 2022c). In other words, Wells turbine rotational speed control affects the OWC hydrodynamic performance and, therefore, rotational speed can, and should, be modulated to improve the overall wave-to-wire (W2W) efficiency of the OWC system (as opposed to maximise only turbine efficiency). Finally, alongside hydrodynamic and turbine performance, also the characteristics of the electric generator should also be considered in the complete W2W system.

In this paper, important steps towards W2W control of OWC systems, through Wells turbine rotational speed modulation, are made. In general, the W2W control problem can be tackled in two different ways. One way is to solve an online nonlinear constrained optimisation problem. Some solutions to such W2W control problems for OWCs (Silva et al., 2023) and other floating WEC types (Haider et al., 2021; Bacelli and Ringwood, 2014) have emerged, but the resulting real-time optimisation problems are quite nasty and, in many cases, convexity is not guaranteed. Furthermore, typical nonlinear WEC controllers can handle only specific types of nonlinearity, related to hydrodynamic models of floating bodies, while the main source of nonlinearity in OWC modelling is the turbine. In contrast to the global optimisation approach, the W2W control strategy considered in this paper follows a somewhat more traditional (García-Violini et al., 2020) and simpler method based on static efficiencies, which allows for a direct comparison with the specific turbine efficiency maximising control approach. In particular, the effect of turbine rotational speed on the OWC W2W performance is analysed, and a possible generator power curve for W2W efficiency maximisation is obtained by solving a static optimisation problem. Results from numerical simulation, carried out in different sea states, for a Mutriku-like (Torre-Enciso et al., 2009) fixed OWC device equipped with a Wells turbine, show that hydrodynamic performance is significantly affected by rotational speed. As such, electric energy production significantly improves if turbine rotational speed is controlled considering the complete OWC system, rather than just the turbine.

The paper structure is organised as follows. In Section 2, the W2W model of the fixed OWC considered in the numerical simulation is presented. In Section 3, numerical simulation is carried out to investigate the effect of rotational speed on the OWC W2W performance. Furthermore, a generator power curve for maximising W2W efficiency is proposed. Results of the numerical simulations, and co-design aspects, are discussed in Section 4. Finally, some conclusive remarks are provided in Section 5.

2. OWC MODELLING

A physics-based model of the Mutriku-like fixed OWC WEC considered in this paper is now presented, and, to simplify the notation, the time dependence of variables is omitted. The values of the parameters of the OWC system are detailed in Table 1 (Henriques et al., 2019).

Table 1. OWC system parameters

m_p	27748	(kg)	$A(\infty)$	71618	(kg)
I	3.06	(kg m^2)	S_w	19.35	(m^2)
d_r	0.75	(m)	l	4.5	(m)
κ	0.775	(-)	V_0	144	(m^3)

2.1 Hydrodynamic modelling

Under liner potential theory assumptions, if the water column is modelled as a neutrally buoyant piston, the hydrodynamic model for a fixed OWC can be written (Evans, 1978) as

$$m_\mathrm{p}\dot{v} = -\rho_\mathrm{w} g S_\mathrm{w} z - S_\mathrm{w} p_\mathrm{c} - f_\mathrm{r} + f_\mathrm{ex}, \tag{2}$$

where m_p is the piston mass, z is the position of the water column relative to the still water level, $v = \dot{z}$ is the velocity of the water column, ρ_w is the water density, g is the gravity acceleration constant, S_w is the OWC water plane area, p_c is the air chamber pressure, f_ex indicates the excitation force due to an incident wave of frequency ω, and f_r is the force due to radiated waves, written as

$$f_\mathrm{r} = A(\infty)\dot{v} + \int_{-\infty}^{t} k_\mathrm{r}(t-\tau)\, v(\tau)\, \mathrm{d}\tau. \tag{3}$$

In Eq. (3), $A(\infty)$ is the OWC added mass at infinite frequency ($A(\omega)|_{\omega\to\infty} = A(\infty)$), while k_r is the piston impulse response function computed as the inverse Fourier transform of the OWC radiation damping, $B(\omega)$. Finally, the excitation force is computed as a sum of N components of frequency ω_n (Henriques et al., 2019), as

$$f_\mathrm{ex} = \sum_{\mathrm{n}=1}^{N} A_\mathrm{ex}(\omega_\mathrm{n}) \cos(\omega_\mathrm{n}\, t + \phi_\mathrm{ex}(\omega_\mathrm{n})), \tag{4}$$

where A_ex and ϕ_ex are, respectively, the amplitude and phase of the excitation force. The frequency dependent functions $A(\omega)$, $B(\omega)$, $A_\mathrm{ex}(\omega)$, and $\phi_\mathrm{ex}(\omega)$ are obtained by solving a boundary element problem (Falnes, 2002). To this end, the WAMIT software (Ewman and Lee, 2016) is used. The frequency dependant parameters used in this paper are shown in Henriques et al. (2019).

Following a common practice in the wave energy field, the convolution integral in Eq. (3) is approximated with a suitable (and less computationally expensive) linear state space model using, among different possible methods, a Prony method (Sheng et al., 2015).

2.2 Pneumatic chamber modelling

The pressure oscillations in the air chamber can be modeled as

$$\frac{\dot{p}_\mathrm{c}}{p_\mathrm{c}} = -\frac{\gamma}{V_\mathrm{c}}\left(\dot{V}_\mathrm{c} + \frac{w_\mathrm{turb}}{\rho_\mathrm{c}}\right), \tag{5}$$

where $V_\mathrm{c} = V_0 - S_\mathrm{w} z$ is the chamber air volume, V_0 is the air volume in still water conditions, γ is the air specific heat ratio, w_turb indicates the turbine air mass flow rate (positive for outward air flow), and ρ_c is the air chamber density. If the air compression/decompression process is isentropic, $\rho_\mathrm{c} = \rho_0 (p_\mathrm{c}/p_0)^{1/\gamma}$, where the subscript '0' refers to standard atmosphere values.

2.3 Turbine/generator set modelling

If the bearing friction loss is ignored, the turbine/generator set dynamic is modelled as

$$\frac{\mathrm{d}}{\mathrm{d}t}\left(\frac{1}{2} I \Omega^2\right) = P_\mathrm{turb} - P_\mathrm{ctrl} = P_\mathrm{turb} - T_\mathrm{ctrl}\,\Omega, \tag{6}$$

where Ω is the turbine rotational speed, I is the inertia moment of the rotating parts, P_turb is the turbine power, P_ctrl is the generator control power, and T_ctrl is the generator control torque. The electric power in the numerical simulation is computed from the efficiency curve of the squirrel-cage induction generator

Air turbine modelling For large Reynolds numbers (Re $> 10^6$) and small Mach numbers (Ma < 0.3), the dimensionless functions

$$\Phi = f_\Phi(\Psi),\ \Pi = f_\Pi(\Psi), \tag{7}$$

can be used to model the turbine (Dixon and Hall, 2013), where

$$\Phi = \frac{w_\mathrm{turb}}{\rho_\mathrm{air}\,\Omega\,d_\mathrm{r}^3},\ \Pi = \frac{P_\mathrm{turb}}{\rho_\mathrm{air}\,\Omega^3\,d_\mathrm{r}^5},\ \Psi = \frac{\Delta p}{\rho_\mathrm{air}\,\Omega^2\,d_\mathrm{r}^2}. \tag{8}$$

In Eqs. (7) and (8), Ψ is the dimensionless pressure head, Φ is the dimensionless air mass flow rate, Π is the dimensionless turbine power, d_r is the turbine rotor diameter, $\Delta p = p_\mathrm{c} - p_0$, and $\rho_\mathrm{air} = \max(\rho_\mathrm{c}, \rho_0)$ is the air density. Fig. 2 shows $f_\Phi(\Psi)$, $f_\Pi(\Psi)$, and the turbine efficiency, defined as

$$\eta_\mathrm{turb}(\Psi) = \frac{P_\mathrm{turb}}{P_\mathrm{pneu}} = \frac{f_\Pi(\Psi)}{\Psi\, f_\Phi(\Psi)}, \tag{9}$$

for the Wells turbine considered in this paper. In Eq. (9), $P_\mathrm{pneu} = q_\mathrm{turb}\,\Delta p$ is the pneumatic power available to the turbine, where $q_\mathrm{turb} = w_\mathrm{turb}/\rho_\mathrm{air}$ is the turbine volumetric flow rate.

Turbine damping Turbine damping is defined as the ratio $w_\mathrm{turb}/\Delta p$ and, for a Wells turbine, is a function of the rotational speed (Falcão and Gato, 2012), as

$$\Theta = \frac{w_\mathrm{turb}}{\Delta p} = \frac{d_\mathrm{r}}{\kappa\,\Omega}, \tag{10}$$

where κ is a constant that depends on the turbine geometry. In impulse-like turbines, turbine damping does not depend (or only marginally depends) on Ω (Rosati et al., 2022c), meaning that it is not possible to significantly affect the OWC hydrodynamic performance by modulating Ω. In this paper, since only Wells turbine rotational speed significantly influences hydrodynamic efficiency, a Wells turbine is considered for maximising the W2W efficiency through rotational speed modulation. Fig. 3 shows the relationship between w_turb and Δp, as Ω varies, for different types of self-rectifying air turbines.

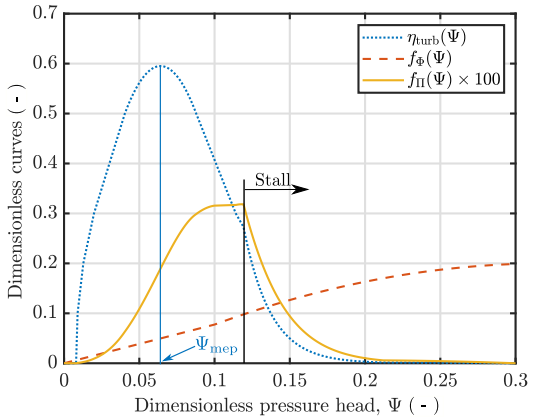

Fig. 2. Φ, Π, and η_turb as functions of Ψ for the Wells turbine considered in this paper.

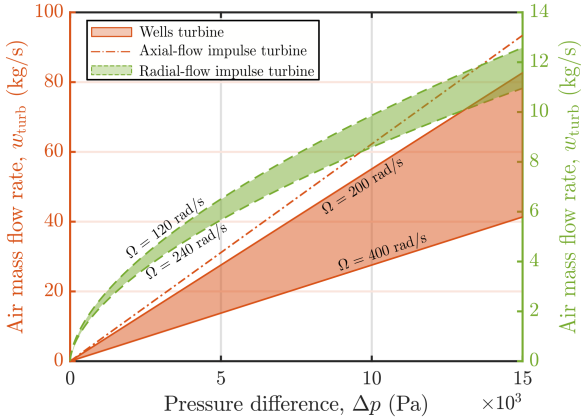

Fig. 3. Pressure difference vs mass flow rate for a Wells turbine with $d_\mathrm{r} = 0.75$ m, and for two different types of impulse turbines, both with $d_\mathrm{r} = 0.65$ m. The air density is considered constant, $\rho_\mathrm{air} = \rho_0$.

3. W2W EFFICIENCY MAXIMISATION

3.1 Effect of turbine rotational speed

The effect of turbine rotational speed on the W2W performance of the Mutriku-like device presented in Section 2 is investigated for fifteen evenly spaced constant values of Ω, ranging from 50 to 400 rad/s. Numerical simulations are run for eight different irregular sea states (SS1-SS8), generated from JONSWAP spectral density functions (Hasselmann et al., 1973) with peak shape parameter $\gamma^\mathrm{J} = 3.3$. The significant wave height, H_s, and peak period, T_p, of the considered sea states (which are selected considering the characteristic wave climate measured at the Mutriku power plant (Torre-Enciso et al., 2009)), are listed in Table

2. To take into account the shoaling effect, characterising the ocean waves at Mutriku power plant, the JONSWAP spectra are modified using an attenuation function, as detailed in Henriques et al. (2019). For all of the 120 tested conditions (15 values of Ω and 8 sea states), 20 distinct realizations are run for 1200 s each, with a time step of 0.01 s.

For each realization, the time-averaged pneumatic power, $\bar{P}_{\text{pneu}}$, turbine power, $\bar{P}_{\text{turb}}$, electric power, $\bar{P}_{\text{elec}}$, and turbine efficiency, $\bar{\eta}_{\text{turb}}$, are computed. Furthermore, the hydrodynamic capture width ratio (CWR), ξ_{hydro}, aerodynamic CWR, ξ_{aero}, and electric CWR, ξ_{elec}, defined as

$$\xi_{\text{hydro}} = \frac{\bar{P}_{\text{pneu}}}{\bar{P}_{\text{wave}}\, l},\ \xi_{\text{aero}} = \frac{\bar{P}_{\text{turb}}}{\bar{P}_{\text{wave}}\, l},\ \xi_{\text{elec}} = \frac{\bar{P}_{\text{elec}}}{\bar{P}_{\text{wave}}\, l} \tag{11}$$

are also calculated. In Eq. (11), l is the OWC capture width and $\bar{P}_{\text{wave}}$, which is a function of the sea state, is the time-averaged wave power per metre of wave crest. ξ_{elec} is essentially the OWC W2W efficiency, ξ_{aero} is the wave-to-mechanical efficiency, and ξ_{hydro} is the wave-to-pneumatic efficiency (or hydrodynamic efficiency). The mean values (from 20 realizations) of the quantities of interest are shown, for three different sea states, in Fig. 4.

Table 2. Parameters of the sea states

Sea state	H_{s} (m)	T_{p} (s)
SS1	0.88	6.40
SS2	1.03	7.55
SS3	1.04	8.75
SS4	1.08	11.05
SS5	1.48	14.55
SS6	1.81	15.70
SS7	2.07	16.90
SS8	3.20	14.55

3.2 Generator power curves

Fig. 5 shows $\bar{P}_{\text{elec}}$ (the blue curves) as a function of Ω for the sea states SS1 - SS8, and two different generator control laws. The green dashed curve is a turbine efficiency maximising control law, while the orange curve is a proposed control law for W2W efficiency maximisation.

A turbine efficiency maximising control law, introduced by Justino and Falcão (1999), has the following form

$$P_{\text{ctrl}} = T_{\text{ctrl}}\,\Omega = a_1\,\Omega^{a_2}. \tag{12}$$

To maximise turbine efficiency, the turbine is operated at its maximum efficiency point, i.e. Ψ_{mep} (see Fig. 2). To this end, the control parameters in Eq. (12) are set as $a_1 = \rho_{\text{air}}\, d_{\text{r}}^5\, f_{\Pi}(\Psi_{\text{mep}})$ and $a_2 = 3$, where a_1 is approximately constant since $\rho_{\text{air}} \approx \rho_0$. For the Wells turbine considered in this paper, $a_1 = 3 \times 10^{-4}$.

To maximise the W2W efficiency, a possible control law for the generator is found by fitting a suitable curve to the peak values of $\bar{P}_{\text{elec}}$. For the OWC system considered in this paper, a suitable control curve is of the type

$$P_{\text{ctrl}} = T_{\text{ctrl}}\,\Omega = \underbrace{b_1 + b_2\,\Omega}_{\text{linear term}} + \underbrace{c_1\,\exp^{c_2\,\Omega}}_{\text{exponential term}}, \tag{13}$$

where $b_1 = 136.088$, $b_2 = 0.739$, $c_1 = 1.151$, and $c_2 = 0.0337$. The linear term determines the value of P_{ctrl} for relatively low values of Ω (< 100 rad/s), while the exponential term becomes the dominant term if Ω is relatively high (> 200 rad/s). It should be noted that, in contrast to the turbine efficiency maximising law in Eq. (12), which is derived analytically (Justino and Falcão, 1999), the W2W efficiency maximising law in Eq. (13) is derived purely from data, therefore is specific for the OWC model in Section 2.

Table 3 reports the percentage values of $\bar{\eta}_{\text{turb}}$, ξ_{elec}, and relative increase in electrical power, $\bar{P}^{\%}_{\text{elec}}$, obtained using the two control laws in Eqs. (12) and (13). For each control law, numerical simulations are run for 1200 s with a time step of 0.01 s, and the percentage values in Table 3 are the mean values obtained from 20 sea state realizations.

Table 3. Results of the simulations

	Eq. (12): $\bar{\eta}^{\max}_{\text{turb}}$		Eq. (13): $\xi^{\max}_{\text{elec}}$		
Sea state	$\bar{\eta}_{\text{turb}}$	ξ_{elec}	$\bar{\eta}_{\text{turb}}$	ξ_{elec}	$\bar{P}^{\%}_{\text{elec}}$
SS1	36.8	2.8	29.9	2.8	~ 0
SS2	36.9	4.2	30.4	4.3	~ 0
SS3	37.2	7.8	32.3	8.0	2.0
SS4	37.7	13.0	35.1	13.3	2.6
SS5	38.5	11.1	37.4	12.2	8.9
SS6	38.7	10.2	38.2	11.7	12.5
SS7	38.8	10.7	38.6	11.0	2.5
SS8	39.1	4.5	37.0	13.7	67.2

4. DISCUSSION

4.1 Results of the numerical simulations

Figure 4 shows that the turbine MEP generally does not coincide with the optimum operating points for the electric generator and/or the hydrodynamic part. To optimise sole turbine performance, since η_{turb} is a function of Ψ (see Fig. 2), Ω should be lower if low pressure levels are available in the chamber (Fig. 4(a)) and vice-versa (Fig. 4(b) and (c)).

Since Wells turbine damping is a function of the rotational speed (see Eq. (10)), hydrodynamic performance (i.e., ξ_{hydro} and P_{pneu}) depend on Ω, particularly when medium-to-high (Fig. 4(b) and (c)) wave energy levels are available. Indeed, with high pressure levels in the pneumatic chamber, variations in Ω have a significant impact on turbine damping (as shown by the 'red cone' in Fig. 3). In general, as Ω increases, Δp tends to increase, whereas q_{turb} decreases. To maximise $\bar{P}_{\text{pneu}}$, a trade-off between Δp and q_{turb} has to be made.

From Table 3, in comparison to the turbine efficiency maximising approach (Eq. (12)), the W2W control approach (Eq. (13)) provides higher values of ξ_{elec}, albeit slightly penalising $\bar{\eta}_{\text{turb}}$. Ultimately, if Ω is modulated, considering the whole OWC system, $\bar{P}_{\text{elec}}$ significantly increases (last column in Table 3) for medium-to-high energy sea states (SS3 - SS8). For SS4, ξ_{elec} is particularly high since T_{p} of SS4 is close to a resonance period of the Mutriku plant (Henriques et al., 2019) and, therefore, ξ_{hydro} is relatively high if Ω is appropriately controlled (see Fig. 4(b)). Furthermore, since the green dashed curve almost intersects the orange curve at SS7 (see Fig. 5), the performance obtained with Eqs. (12) and (13) is similar for SS7 (see Table 3).

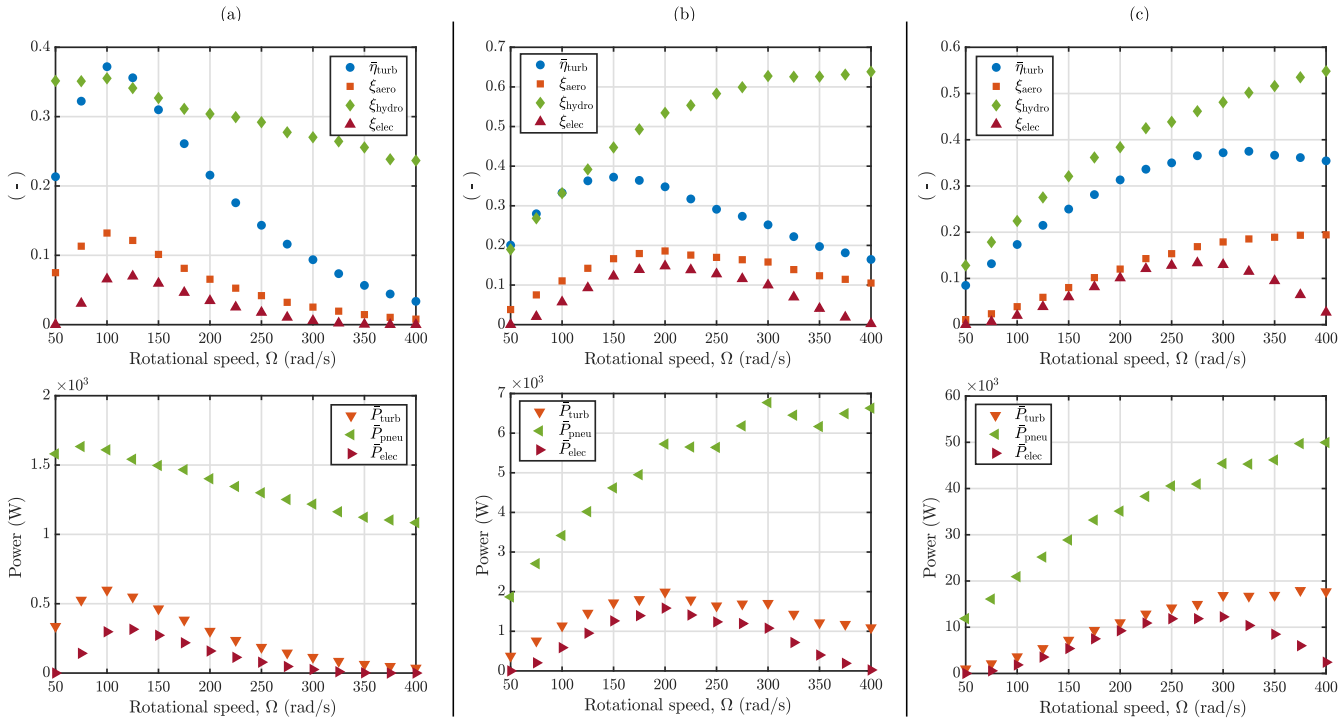

Fig. 4. Effect of Ω on the OWC system performance for three sea states: (a) SS1, (b) SS4, and (c) SS8.

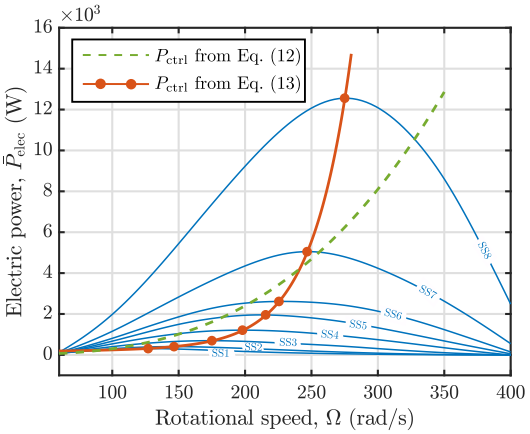

Fig. 5. The blue curves represent $\bar{P}_{elec}$ as a function of Ω for different sea states. The two control curves from Eqs. (12) and (13) are also shown.

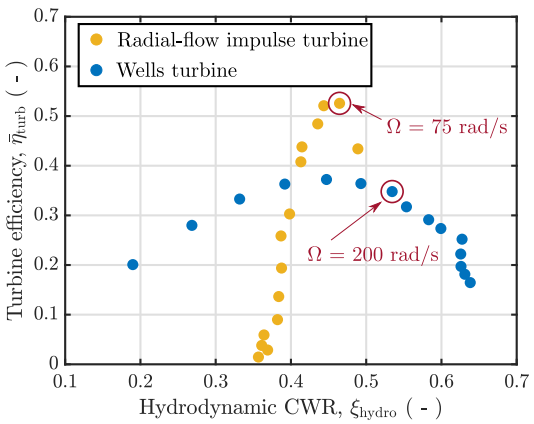

Fig. 6. Values of ξ_{hydro} and $\bar{\eta}_{turb}$ for different values of Ω, in sea state SS4. For each turbine type, the red circles highlight the cases in which ξ_{turb} is maximised.

4.2 Elements of co-design

In WEC geometry optimisation, control-related aspects should be considered from an early WEC design stage. To this end, control co-design techniques significantly help to achieve the optimum *control-informed* WEC design (Garcia-Rosa et al., 2015). Therefore, it is worth highlighting some key co-design aspects.

As already stated, W2W efficiency maximisation, through modulation of Ω, requires a specific turbine, namely a Wells turbine, which is frequently used on OWCs (see Table 1 in Rosati et al. (2022b)). Fig. 6 shows, for two different types of turbine, the values of ξ_{hydro} and $\bar{\eta}_{turb}$ obtained in SS4, for different constant values of Ω. In comparison with the Wells turbine case, the variation of ξ_{hydro} with Ω is small for the radial-flow impulse turbine (the model for which can be found in Rosati et al. (2022c)), meaning that hydrodynamic performance is only moderately affected by variations in Ω and, consequently, W2W efficiency maximisation through turbine rotational speed modulation is less effective. The two red circles indicate the condition in which ξ_{turb} is maximised, hence the case in which the best trade-off between turbine and hydrodynamic performance is achieved. For the radial-flow impulse turbine, due to the the poor effect of Ω on ξ_{hydro}, the condition in which ξ_{turb} is maximised is the condition in which $\bar{\eta}_{turb}$ is maximum.

To maximise the benefit of W2W efficiency maximisation for OWC WECs, a Wells turbine with a relatively flat efficiency curve should be designed/selected. Indeed, with a relatively high-valued and flat turbine efficiency curve, Ω could be modulated to improve hydrodynamic perfor-

mance more freely, without risking excessive penalisation of turbine efficiency. In other words, the control envelope (possibility) for Ω increases. On the other hand, if the Wells turbine efficiency curve is too peaky, rotational speed control should prioritize turbine performance; otherwise, unsatisfactory levels of produced energy are obtained.

5. CONCLUSION

In light of the discussion in Section 4, all the energy conversion processes of an OWC system equipped with a Wells turbine are affected by rotational speed control. As such, electric energy production can be significantly improved if rotational speed is controlled while considering the complete W2W OWC system. Furthermore, co-design aspects are vital for maximising the benefit of W2W control for OWC systems.

In this paper, control constraints (Rosati et al., 2022c), power losses due to friction and viscosity, grid-side control and power quality aspects (Said and Ringwood, 2021), and possible reference tracking issues that may arise in real-time control applications are not considered. In real-time control applications, pressure (Marques Silva et al., 2021) or free surface elevation forecasting (Paparella et al., 2015) may also be required for anticipating the control action.

REFERENCES

Astariz, S. and Iglesias, G. (2015). The economics of wave energy: A review. *Renew. Sust. Energ. Rev.*, 45, 397–408.

Bacelli, G. and Ringwood, J.V. (2014). Nonlinear optimal wave energy converter control with application to a flap-type device. In *Proc. IFAC World Congress*, volume 47, 7696–7701. Cape Town, South Africa.

Chang, G., Jones, C.A., Roberts, J.D., and Neary, V.S. (2018). A comprehensive evaluation of factors affecting the levelized cost of wave energy conversion projects. *Renew. Energy*, 127, 344–354.

Dixon, S.L. and Hall, C. (2013). *Fluid mechanics and thermodynamics of turbomachinery*. Butterworth-Heinemann.

Evans, D.V. (1978). The oscillating water column wave-energy device. *IMA J. Appl. Math.*, 22(4), 423–433.

Ewman, J.N. and Lee, C.H. (2016). WAMIT user manual. URL `http://www.wamit.com/manual.htm`. Last accessed 02 March 2019.

Falcão, A.F.O. and Gato, L.M.C. (2012). Air turbines. In A. Sayigh (ed.), *Comprehensive Renewable Energy*, volume 8, 111–149. Elsevier, Oxford.

Falcão, A.F.O. and Henriques, J.C.C. (2016). Oscillating-water-column wave energy converters and air turbines: A review. *Renew. Energy*, 85, 1391–1424.

Falnes, J. (2002). *Wave Interaction with Oscillating Water Columns*, 225–262. Cambridge University Press.

Garcia-Rosa, P.B., Bacelli, G., and Ringwood, J.V. (2015). Control-informed geometric optimization of wave energy converters: The impact of device motion and force constraints. *Energies*, 8(12), 13672–13687.

García-Violini, D., Faedo, N., Jaramillo-Lopez, F., and Ringwood, J.V. (2020). Simple controllers for wave energy devices compared. *J. Mar. Sci. Eng.*, 8(10), 793.

Garrido, A.J., Garrido, I., Amundarain, M., Alberdi, M., and De la Sen, M. (2012). Sliding-mode control of wave power generation plants. *IEEE Trans. Ind. Appl.*, 48(6), 2372–2381.

Haider, A.S., Brekken, T.K., and McCall, A. (2021). Application of real-time nonlinear model predictive control for wave energy conversion. *IET Renew. Power Gener.*, 15(14), 3331–3340.

Hasselmann, K., Barnett, T.P., Bouws, E., Carlson, H., Cartwright, D.E., Enke, K., Ewing, J.A., Gienapp, A., Hasselmann, D.E., Kruseman, P., et al. (1973). Measurements of wind-wave growth and swell decay during the joint north sea wave project (JONSWAP). *Deutches Hydrographisches Institut*.

Henriques, J.C.C., Portillo, J.C.C., Sheng, W., Gato, L.M.C., and Falcão, A.F.O. (2019). Dynamics and control of air turbines in oscillating-water-column wave energy converters: Analyses and case study. *Renew. Sust. Energ. Rev.*, 112, 571–589.

Justino, P.A.P. and Falcão, A.F.O. (1999). Rotational Speed Control of an OWC Wave Power Plant. *J. Offshore Mech. Arct. Eng.*, 121(2), 65–70.

Marques Silva, J., Vieira, S.M., Valério, D., Henriques, J.C.C., and Sclavounos, P.D. (2021). Air pressure forecasting for the mutriku oscillating-water-column wave power plant: Review and case study. *IET Renew. Power Gener.*, 15(14), 3485–3503.

Paparella, F., Monk, K., Winands, V., Lopes, M.F.P., Conley, D., and Ringwood, J.V. (2015). Up-wave and autoregressive methods for short-term wave forecasting for an oscillating water column. *IEEE Trans. Sustai.*, 6(1), 171–178.

Ringwood, J.V. (2020). Wave energy control: status and perspectives 2020. In *Proc. IFAC World Congress*. Berlin, Germany.

Rosati, M., Henriques, J.C.C., and Ringwood, J.V. (2022a). Oscillating-water-column wave energy converters: A critical review of numerical modelling and control.

Rosati, M., Henriques, J.C.C., and Ringwood, J.V. (2022b). Oscillating-water-column wave energy converters: A critical review of numerical modelling and control. *Energy Convers. Manag. X*, 16, 100322.

Rosati, M. and Ringwood, J.V. (2022). Towards hydrodynamic control of an oscillating water column wave energy converter. *Trends in Renew. Energ. Offshore*, 411–418.

Rosati, M., Ringwood, J.V., and Henriques, J.C.C. (2022c). A comprehensive wave-to-wire control formulation for oscillating water column wave energy converters. *Trends in Renew. Energ. Offshore*, 329–337.

Said, H.A. and Ringwood, J.V. (2021). Grid integration aspects of wave energy—overview and perspectives. *IET Renew. Power Gener.*, 15(14), 3045–3064.

Sheng, W., Alcorn, R., and Lewis, A. (2015). A new method for radiation forces for floating platforms in waves. *Ocean Engineering*, 105, 43–53.

Silva, J.M., Vieira, S.M., Valério, D., and Henriques, J.C. (2023). GA-optimized inverse fuzzy model control of OWC wave power plants. *Renew. Energ.*

Torre-Enciso, Y., Ortubia, I., De Aguileta, L.I.L., and Marqués, J. (2009). Mutriku wave power plant: From the thinking out to the reality. In *Proc. of the 8th European Wave and Tidal Energy Conference*, 319–329. Uppsala, Sweden.